

EXPERIMENTAL RESULTS ON A PLANAR ARRAY OF PARASITIC DIPOLES FED BY ONE ACTIVE ELEMENT

M. Álvarez-Folgueiras, J. A. Rodríguez-González
and F. Ares-Pena

Department of Applied Physics, Faculty of Physics
University of Santiago de Compostela
Santiago de Compostela 15782, Spain

Abstract—A planar array composed of 41 parasitic dipoles above a ground plane, fed by an active dipole at 5 GHz, was designed to obtain a pencil beam pattern with a moderate gain and bandwidth. Experimental results are in good agreement with the theory and show a pattern with an 18.78 dB gain, a sidelobe level (SLL) of -15 dB, an impedance bandwidth of 16.53% (the frequency range over which the value of S_{11} is below -10 dB) and a 2.7% bandwidth that is achieved within 1 dB gain variations.

1. INTRODUCTION

Recently a technique was described for designing a planar array of parasitic dipoles that modify the pattern of a $\lambda/2$ -dipole placed $\lambda/4$ over a ground plane, in order to obtain a pencil beam with good performance [1]. The method uses Particle Swarm Optimization (PSO) [2–12] to optimize the length of each parasitic dipole and the distance between the planar array and the ground plane as well as the interspacing of the parasitic elements [13–19] (Figure 1). This radiating system works as a set of scattering elements in a mutual coupling environment localized in a plane. Each element, in the presence of others, acquires a phased-up trans-scattering capability. Similar configurations have been proposed [20, 21], based on a Fabry-Perot antenna with a partially reflective surface (PRS). However, the bandwidth and efficiency are usually reduced with this kind of antenna. In addition, the antenna described in [21] requires three PRS layers to

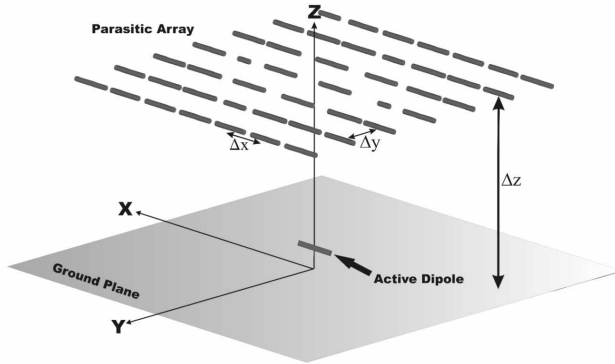


Figure 1. Geometry of the antenna, composed of a planar array of parasitic dipoles fed by an active dipole and backed by a ground plane.

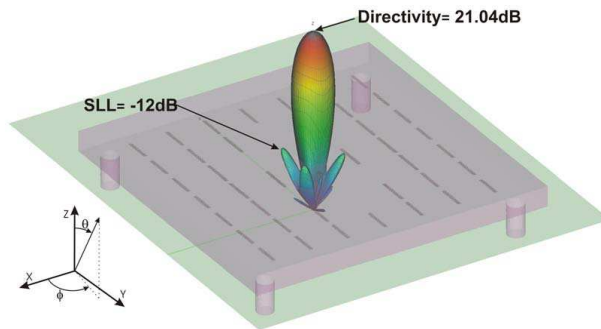


Figure 2. Power pattern simulated by the antenna composed of 41 parasitic elements placed 0.59λ in front of a finite ground plane; the dielectric substrate and the Teflon screws have been taken into account.

maximize the gain, which reduces antenna compactness. In this study, an experimental test of a planar array with 41 parasitic elements was carried out. The construction of the array and the experimental results are discussed here.

2. CONSTRUCTION

The design of the antenna is found in [1]. The antenna is composed of 41 parasitic elements, after the removal of 8 elements with practically null currents (current density less than 2.25 A/m). After the optimization process had been completed, the antenna had a directivity of 21.04 dB and a SLL of -12 dB , with $\Delta z = 0.59\lambda$, $\Delta y = 0.6\lambda$, and

$\Delta x = 0.55\lambda$ (Figure 2). The final size of the antenna was $4.73\lambda \times 4.6\lambda$, including a finite ground plane $\lambda/2$ larger than the parasitic array in each direction. In this simulation, the electrical characteristics of the different parts of the antennas were taken into account.

2.1. Feeder

For the construction of the feeder, a dipole with two asymmetric arms (each one printed on one side of the dielectric substrate) was selected and set $\lambda/4$ above the ground plane. With this simple design the current could be balanced over the arms of the dipole. The feeder design was simulated and optimized by FEKO [22] (using its internal Down-Hill simplex local optimization algorithm) in order to obtain the best performance at the specified frequency. In the optimization process, the length and the width of each arm were modified to obtain a correct match at the design frequency and improve the performance of the dipole.

After completing the optimization process the feeder was adapted to 5 GHz. The final size of the feeder is presented in Figure 3. The length of the dipole arms were 0.18λ and 0.21λ and the width was 0.083λ (5 mm), yielding a directivity of 8.3 dB.

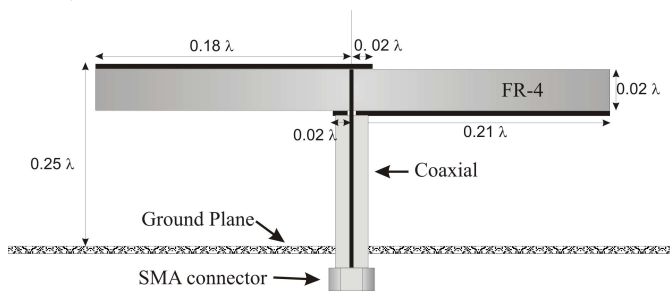


Figure 3. Dipole geometry.

The dipole was printed over a 1.5 mm thick FR-4 ($\epsilon_r = 4.6$, $\tan \delta = 0.014$) double-sided copper substrate. To keep it at the correct distance over the ground plane, the dipole was soldered to a rigid coaxial that goes through the ground plane and ends in an SMA connector for hook-up to the measurement equipment; see Figure 4.

2.2. Parasitic Array

The DICLAD 880 ($\epsilon_r = 2.7$, $\tan \delta = 0.0009$) was selected on the basis of performance, cost and substrate availability. Given the antenna



Figure 4. Photograph of the feeder fixed and soldered above the ground plane.

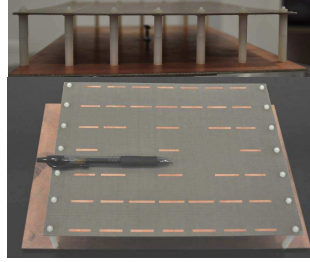


Figure 5. Photograph of the antenna, composed of a planar array of parasitic dipoles fed by an active dipole backed by a ground plane (detail of Teflon screws).

size, we found that a substrate thickness of 0.05 inches was enough to guarantee an acceptable stiffness when the parasitic plane was attached to the ground plane.

The parasitic dipoles above the substrate were milled by rapid PCB prototyping.

Teflon columns were used for assembly of the parasitic array above the ground plane. These columns were arranged on opposite sides of the substrate and could be adjusted to fit the design value for the distance between the array and the ground plane. Finally, the ground plane was drilled and fixed to the parasitic array; see Figure 5.

3. MEASUREMENT

The measurement process was developed in the anechoic chamber at the University of Santiago de Compostela. It is a shielding enclosure of $8.5 \times 4.5 \times 4.5$ m ($L \times W \times H$) and is lined with a combination of 8 and 18 inch pyramidal microwave absorbers to ensure a reflectivity better than -30 dB above 1 GHz.

The positioner for testing the antenna is a roll/polarization mast. The antenna under the test positioner is also a roll/polarization mounted on a mast but equipped with a slide to align the phase centre. This slide is installed on an azimuth positioner that is mounted on a manual slide and can move linearly along the Z axis.

3.1. Feeder

In Figures 6 and 7 the copolar power patterns measured and simulated for the $\Phi = 0^\circ$ and $\Phi = 90^\circ$ planes, respectively, are

presented. The measured crosspolar component is also shown. The tolerable differences between both are attributed to imperfection in the construction process. The directivity was 8.3 dB for the simulation vs. 8.0 dB, which was calculated by integrating the measured 3D pattern, using the available software. The measured gain of the antenna was 7.79 dB (calculated using the Gain-Transfer method).

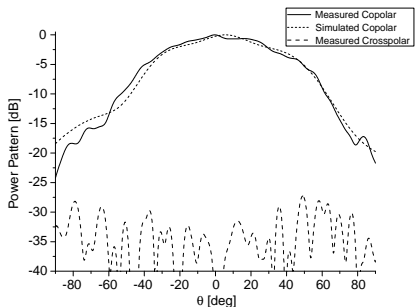


Figure 6. Power pattern of the feeder dipole for $\Phi = 0^\circ$. Solid line: Copolar measured results; Dotted line: Copolar simulated results; Broken line: Crosspolar measured results.

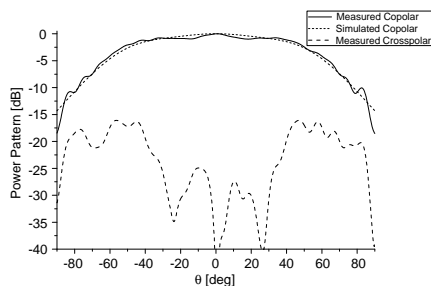


Figure 7. Power pattern of the feeder dipole for $\Phi = 90^\circ$. Solid line: Copolar measured results; Dotted line: Copolar simulated results; Broken line: Crosspolar measured results.

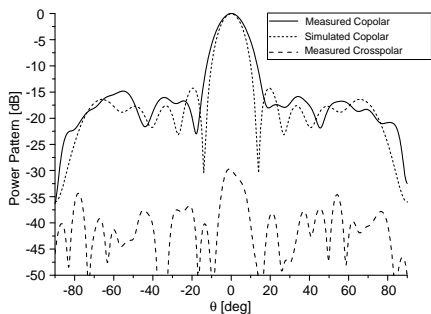


Figure 8. Power pattern of the antenna for $\Phi = 0^\circ$. Solid line: Copolar measured results; Dotted line: Copolar simulated results; Broken line: Crosspolar measured results.

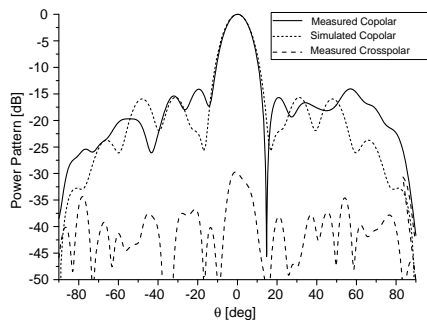


Figure 9. Power pattern of the antenna for $\Phi = 90^\circ$. Solid line: Copolar measured results; Dotted line: Copolar simulated results; Broken line: Crosspolar measured results.

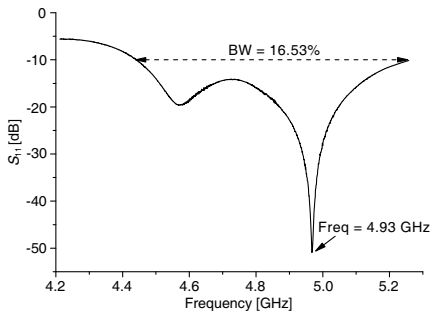


Figure 10. Measured magnitude of the input reflection coefficient of the complete antenna.

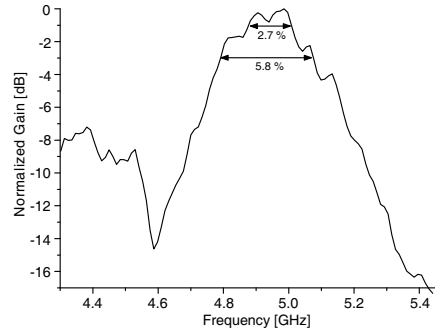


Figure 11. Measured gain bandwidth.

3.2. Final Antenna

After the measurement process, the antenna showed a directivity of 19.62 dB (calculated by integrating the measured 3D pattern as above) and an SLL of -15 dB. The antenna gain obtained by the gain-transfer method was 18.78 dB, which corresponds to an efficiency of 82.42%. Figures 8 and 9 show the comparison between the measured copolar power pattern and the FEKO simulated pattern [22] along with the measured crosspolar component for $\Phi = 0^\circ$ and $\Phi = 90^\circ$, respectively. The crosspolar component value was -30 dB under the copolar power pattern in the transmission zone. Measurement of the input reflection coefficient, S_{11} , revealed a bandwidth of 16.53% at -10 dB, (Figure 10), with a resonance frequency of 4.93 GHz. A 5.8% and a 2.7% bandwidth were achieved within 3 dB and 1 dB gain variations, respectively (Figure 11). The frequency shifted from 5 GHz to 4.93 GHz due to losses, inaccuracies and materials used in the manufacturing process. Note that the antenna described in [20] using a PRS of $5\lambda \times 5\lambda$ above a ground plane of $10\lambda \times 10\lambda$, shows a -3 dB gain bandwidth of 1.3%, a -10 dB S -parameter bandwidth of approximately 1.05%, and an efficiency of about 54%.

4. CONCLUSIONS

The experiment verified the good performance of a 41 parasitic dipole array fed by a single active dipole radiating in a pencil beam pattern. The results measured from the constructed model show tolerable discrepancies with the simulated results. These differences result from inaccuracy in the construction process, interactions of the materials used and soldering imperfections.

ACKNOWLEDGMENT

This work has been supported by the Spanish Ministry of Education and Science under Project TEC2008-04485 and by the Xunta de Galicia under Project 09TIC006206PR.

REFERENCES

1. Alvarez Folgueiras, M., J. A. Rodriguez Gonzalez, and F. J. Ares-Pena, "Pencil beam patterns obtained by planar arrays of parasitic dipoles fed by only one active element," *Progress In Electromagnetics Research*, Vol. 103, 419–431, 2010.
2. Carro Ceballos, P. L., J. De Mingo Sanz, and P. G. Dúcar, "Radiation pattern synthesis for maximum mean effective gain with spherical wave expansions and particle swarm techniques," *Progress In Electromagnetics Research*, Vol. 103, 355–370, 2010.
3. Barkat, O. and A. Benghalia, "Synthesis of superconducting circular antennas placed on circular array using a particle swarm optimisation and the full-wave method," *Progress In Electromagnetics Research B*, Vol. 22, 103–119, 2010.
4. Pathak, N. N., G. K. Mahanti, S. K. Singh, J. K. Mishra, and A. Chakraborty, "Synthesis of thinned planar circular array antennas using modified particle swarm optimization," *Progress In Electromagnetics Research Letters*, Vol. 12, 87–97, 2009.
5. Mangoud, M. A. and H. M. Elragal, "Antenna array pattern synthesis and wide null control using enhanced particle swarm optimization," *Progress In Electromagnetics Research B*, Vol. 17, 1–14, 2009.
6. Khodier, M. M. and M. Al-Aqeel, "Linear and circular array optimization: A study using particle swarm intelligence," *Progress In Electromagnetics Research B*, Vol. 15, 347–373, 2009.
7. Benedetti, M., R. Azaro, and A. Massa, "Memory enhanced PSO-based optimization approach for smart antennas control in complex interference scenarios," *IEEE Trans. Antennas Propagat.*, Vol. 56, 1939–1947, Jul. 2008.
8. Benedetti, M., G. Oliveri, P. Rocca, and A. Massa, "A fully-adaptive smart antenna prototype: Ideal model and experimental validation in complex interference scenarios," *Progress In Electromagnetic Research*, Vol. 96, 173–191, 2009.
9. Rocca, P., L. Poli, G. Oliveri, and A. Massa, "Synthesis of time-modulated planar arrays with controlled harmonic radiations,"

- Journal of Electromagnetic Waves and Applications*, Vol. 24, Nos. 5–6, 827–838, 2010.
10. Lizzi, L., F. Viani, R. Azaro, and A. Massa, “A PSO-driven spline-based shaping approach for ultra-wideband (UWB) antenna synthesis,” *IEEE Trans. Antennas Propagat.*, Vol. 56, 2613–2621, 2008.
 11. Zhang, L., F. Yang, and A. Z. Elsherbeni, “On the use of random variables in particle swarm optimizations: A comparative study of Gaussian and uniform distributions,” *Journal of Electromagnetic Waves and Applications*, Vol. 23, Nos. 5–6, 711–721, 2009.
 12. Zhang, S., S.-X. Gong, and P.-F. Zhang, “A modified PSO for low sidelobe concentric ring arrays synthesis with multiple constraints,” *Journal of Electromagnetic Waves and Applications*, Vol. 23, Nos. 11–12, 1535–1544, 2009.
 13. Kamarudin, M. R. and P. S. Hall, “Switched beam antenna array with parasitic elements,” *Progress In Electromagnetics Research B*, Vol. 13, 187–201, 2009.
 14. Yuan, H.-W., S.-X. Gong, P.-F. Zhang, and X. Wang, “Wide scanning phased array antenna using printed dipole antennas with parasitic element,” *Progress In Electromagnetics Research Letters*, Vol. 2, 187–193, 2008.
 15. Zhang, M., Y.-Z. Yin, J. Ma, Y. Wang, W.-C. Xiao, and X.-J. Liu, “A racket-shaped slot UWB antenna coupled with parasitic strips for band-notched application,” *Progress In Electromagnetics Research Letters*, Vol. 16, 35–44, 2010.
 16. Tu, Z.-H., Q.-X. Chu, and Q.-Y. Zhang, “High-gain slot antenna with parasitic patch and windowed metallic superstrate,” *Progress In Electromagnetics Research Letters*, Vol. 15, 27–36, 2010.
 17. Chen, X., G. Fu, S. X. Gong, J. Chen, and X. Li, “A novel microstrip array antenna with coplanar parasitic elements for UHF RFID reader,” *Journal of Electromagnetic Waves and Applications*, Vol. 23, Nos. 17–18, 2491–2502, 2009.
 18. Donelli, M., R. Azaro, L. Fimognari, and A. Massa, “A planar electronically reconfigurable Wi-Fi band antenna based on a parasitic microstrip structure,” *IEEE Antenna Wireless Propagat. Lett.*, Vol. 6, 623–626, 2007.
 19. Zhao, K., S. Zhang, and S. He, “Enhance the bandwidth of a rotated rhombus slot antenna with multiple parasitic elements,” *Journal of Electromagnetic Waves and Applications*, Vol. 24, Nos. 14–15, 2087–2094, 2010.
 20. Feredesidis, A. P. and J. C. Vardaxoglou, “High gain planar

- antenna using optimized partially reflective surfaces,” *IEE Proc. Microw. Antennas Propag.*, Vol. 148, 345–350, 2001.
21. Gardelli, R., M. Albani, and F. Capolino, “Array thinning by using antennas in a fabry-perot cavity for gain enhancement,” *IEEE Trans. Antennas Propag.*, Vol. 54, 1979–1990, 2006.
 22. EM Software and Systems, FEKO Suite 5.4, (www.feko.info), 2008.